GEOPHYSICAL RESEARCH LETTERS, VOL. 28, NO. 13, PAGES 2521-2524, JULY 1, 2001

Localized failure modes in a compactant porous rock

Teng-fong Wong
Department of Geosciences, State University of New York at Stony Brook

Patrick Baud and Emmanuelle Klein
Institut de Physique du Globe, Université de Louis Pasteur, Strasbourg, France

Abstract. Since dilatancy is generally observed as a precursor to brittle faulting and the development of shear localization, attention has focused on how localized failure develops in a dilatant rock. However, recent geologic observations and reassessment of bifurcation theory have indicated that strain localization may be pervasive in a compactant porous rock. The localized bands can be in shear or in compaction, and oriented at relatively high angles (up to 90°) to the maximum compression direction. Here we report microstructural characterization of the spatial distribution of damage in failed samples which confirms that compaction bands and high-angle conjugate shears can develop in sandstones with porosities ranging from 13% to 28%. These failure modes are generally associated with stress states in the transitional regime from brittle faulting to cataclastic ductile flow. The laboratory results suggest that these complex localized features can be pervasive in sandstone formations, not just limited to aeolian sandstone in which they were first documented. They may significantly impact the stress field, strain partitioning and fluid transport in sedimentary formations and accretionary prisms. While bifuraction theory provides an useful framework for analyzing the inception of localization, our data rule out a constitutive model that does not account for the activation of multiple damage mechanisms in the transitional regime.

Introduction

Dilatancy and brittle faulting typically result in shear bands oriented at angles of ~30° to the maximum (compressive) principal stress σ_1 [*Paterson*, 1978; *Scholz*, 1990]. A fundamentally different failure mode develops if the porous material is stressed under relatively high confinement. The pore space compacts and ductile failure develops with damage distributed in a delocalized manner [*Handin et al.*, 1963; *Wong et al.*, 1997]. Since the brittle-ductile transition is manifested by the concomitant inhibition of dilatancy and shear localization, attention has focused on strain localization that occurs in a dilatant rock. Indeed, in their seminal work on bifurcation analysis of shear localization, *Rudnicki and Rice* [1975] implicitly neglected the possibility that a compactant porous material may fail in a localized mode. However, localized failure has been observed in compactant porous rocks and cellular materials. In particular, "compaction bands" oriented at very high angles of ~90° to σ_1 have recently been observed in the Castlegate sandstone with a porosity of 28% [*Olsson*, 1999; *DiGiovanni et al.*, 2000; *Olsson and Holcomb*, 2000]. Analogous failure was also documented in aluminum and polycarbonate honeycombs [*Papka and Kyriakides*, 1998; 1999].

While there are other types of localized structures that are oriented subnormal to σ_1, it should be noted that the operative deformation mechanisms are distinctly different. In a mature strike-slip fault (such as the San Andreas system), it is attributed to mechanical weakness in both absolute and relative senses [*Rice*, 1992; *Hickman et al.*, 1995]. Pressure solution may also induce stylolites to develop as discrete surfaces oriented normal to σ_1 [*Fletcher and Pollard*, 1981] Since these localized compactant structures can act as barriers to fluid transport and influence the stress field and strain partitioning in accretionary prisms and sedimentary formations [*Mollema and Antonellini*, 1996; *Bryne et al.*, 1993], an important question is to what extent and under what conditions they would occur.

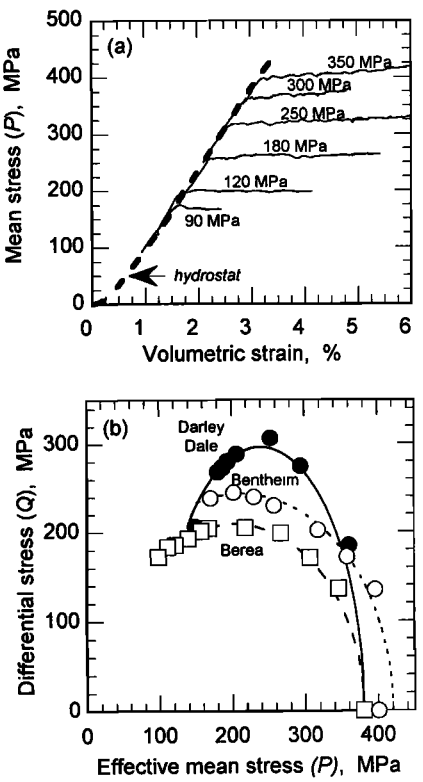

Figure 1. (a) Mean stress as a function of volumetric strain of nominally dry Bentheim sandstone. The triaxial compression experiments were conducted at confining pressures indicated. For reference, the hydrostat is shown as the dashed curve. (b) Yield stresses at the onset of shear-enhanced compaction for Darley Dale, Bentheim and Berea sandstones. The data were fitted with elliptical yield envelopes [*Wong et al.*, 1997; *Baud et al.*, 2000].

Paper number 2001GL012960.
0094-8276/01/2001GL012960$05.00

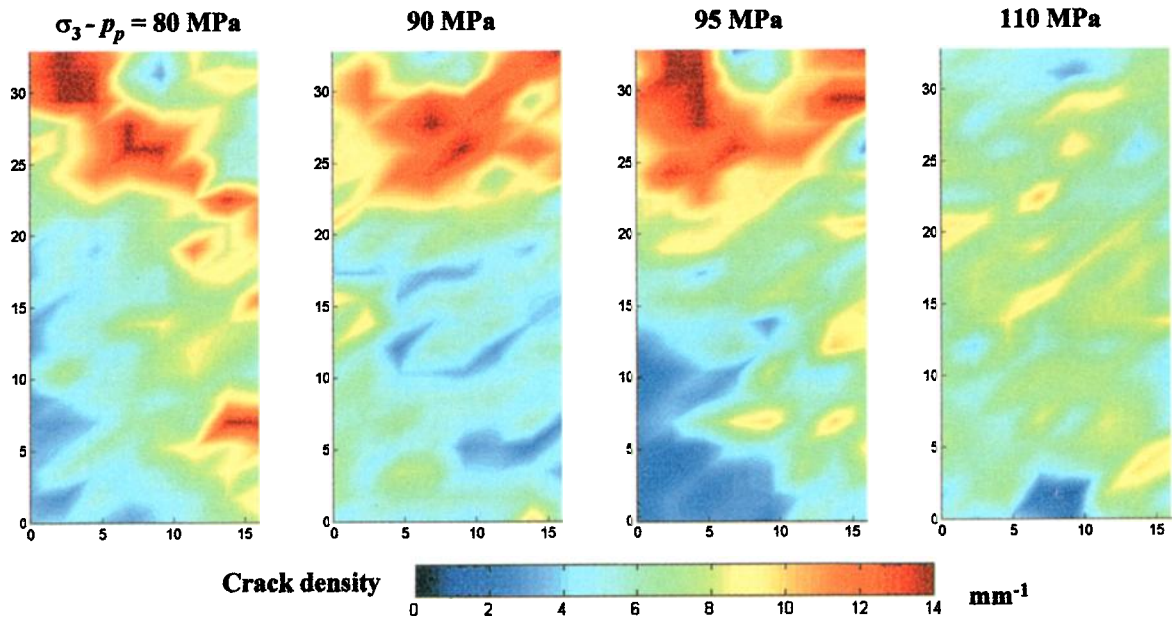

Figure 2. Spatial distribution of damage in Darley Dale sandstone samples deformed to just beyond the onset of shear-enhanced compaction. The saturated samples were deformed at pore pressure of 10 MPa and effective pressures as indicated. The maximum axial strains were 3.0% (at 80 MPa), 2.7% (at 90 MPa), 3.7% (at 95 MPa), and 3.6% (at 110 MPa). Principal stress σ_1 was along the axial direction. The spatial scales of the samples are in mm, and the crack density is specific crack surface area per unit volume inferred from sterological measurements.

To address this question, we conducted a laboratory study on the Bentheim, Berea, and Darley Dale sandstones with porosities of 13%, 21% and 23%, respectively. Since previous work has documented the brittle and ductile end-members [*Wong et al.*, 1997; *Menéndez et al.*, 1996; *Wu et al.*, 2000; *Klein et al.*, 2001], we focus here on the transitional regime to elucidate the constitutive behavior and damage evolution that culminate in localized failure while the sandstone compacts. Our observations demonstrate the prevalence of such localized failure, and the mechanical data provide stringent constraints on the constitutive model that can adequately describe strain localization as a bifurcation phenomenon in a compactant porous rock.

Mechanical and microstructural data

The experiments were conducted in the conventional triaxial configuration, with the principal stresses given by $\sigma_1 > \sigma_2 = \sigma_3$. The Berea and Darley Dale sandstone samples were saturated with distilled water and maintained at a constant pore pressure p_p=10 MPa, whereas the Bentheim sandstone samples were deformed under nominally dry condition, using methodologies described previously [*Wong et al.*, 1997; *Baud et al.*, 2000].

Bentheim sandstone data for the mean stress $P=(\sigma_1+\sigma_2+\sigma_3)/3$ as function of volumetric strain are presented in Figure 1a. For reference, hydrostatic compaction data are also shown. Initially at the application of differential stress ($Q=\sigma_1-\sigma_3$) the volume change was identical to that under hydrostatic loading, implying that the deviatoric stress field did not contribute to compaction. For instance, data for the triaxial compression experiment at confining pressure of 180 MPa show that the volumetric strain was identical to the hydrostat for $P \leq 257.5$ MPa, but beyond this critical stress level (P=257.5 MPa, Q=230.2 MPa), the nonhydrostatic loading significantly enhanced compaction. Typically the sample strain hardens while this phenomenon of "shear-enhanced compaction" occurs. The critical stress levels at the onset of such yielding map

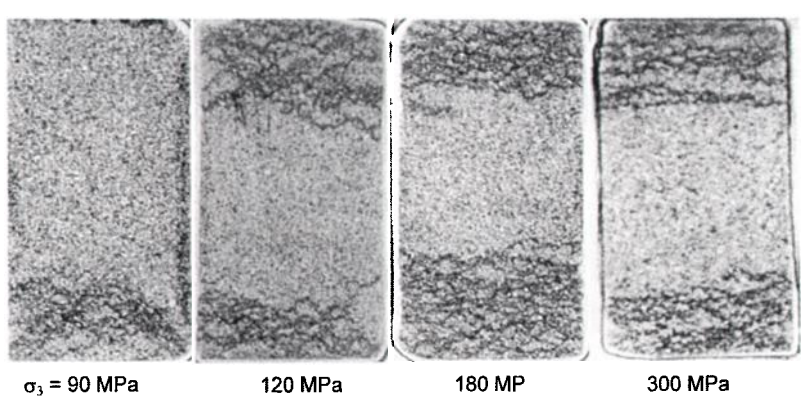

Figure 3. Transmission optical micrographs of Bentheim sandstone samples deformed to just beyond the onset of shear-enhanced compaction. The confining pressures were as indicated. The maximum axial strains were 2.8% (at 90 MPa), 3.5% (at 120 MPa), 4.0% (at 180 MPa), and 3.0% (at 300 MPa). The dark bands are associated with significant comminution. The width of each thin section is ~18 mm. Principal stress σ_1 was along the axial direction.

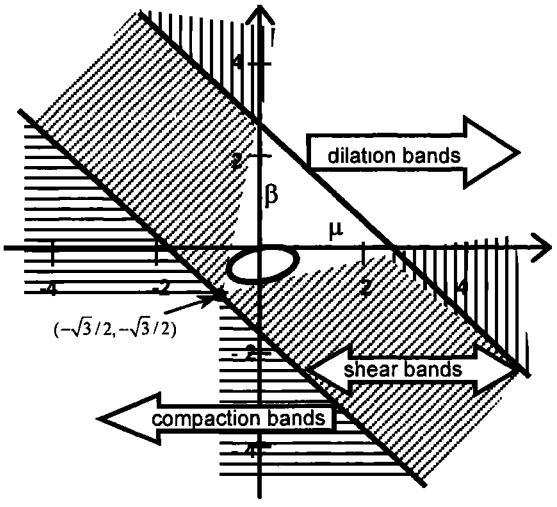

Figure 4. Failure mode map derived from bifurcation analysis of a constitutive model with one yield surface (from *Issen and Rudnicki* [2000]). The three failure modes (compaction band, shear band and dilation band) are separated by the diagonal lines $\beta+\mu=-\sqrt{3}$ and $\beta+\mu=\sqrt{3}(2-\nu)/(1+\nu)$, where ν is Poisson's ratio. For each mode, localization develops during strain hardening in the darkened area and during softening in the unmarked area. The oval near the origin brackets our data for the Bentheim, Berea and Darley Dale sandstone samples that failed by development of compaction or high-angle conjugate shear bands.

out an initial yield envelope in the stress space (Figure 1b). Shear-enhanced compaction was observed only at sufficiently high confinement. Guided by the yield envelopes, sandstone samples were deformed to just beyond the onet of compactive yield, unloaded and retrieved from the pressure vessel. Microstructural observations were then conducted on thin sections of the deformed specimens.

Shear-enhanced compaction is manifested by intensive grain crushing and pore collapse [*Menéndez et al.*, 1996]. Spatial distribution of damage (in terms of intragranular crack density and specific surface area) in the failed samples was characterized using stereological techniques [*Wu et al.*, 2000]. Development of an elongate, connected cluster of anomalous damage that cuts through the sample can be considered as a proxy for localized failure. The damage due to compactive yield in Darley Dale sandstone is illustrated in Figure 2 for four samples. At the effective pressure of 80 MPa, a shear band developed at ~45° in the failed sample. A previous study by *Wu et al.*, [2000] showed that a dilatant sample that failed at relatively low confinement (10 MPa) had a shear band at ~30°. When the effective pressure was increased to 90 MPa and 95 MPa, mosaics of high-angle shear and compaction bands were observed. These bands often developed near one end of the sample. At 110 MPa the clusters of damage became delocalized, with a ductile failure mode analogous to that at 200 MPa [*Wu et al.*, 2000].

Our Berea sandstone samples show qualitatively similar features in the transitional regime, with a complex hybrid of high-angle conjugate shears and compaction bands in samples that failed at effective pressures of 40-150 MPa. For the Bentheim sandstone (Figure 3) high-angle conjugate shears were observed at a confining pressure of 90 MPa, but at higher pressures from 120 to 300 MPa, unequivocal development of compaction bands was observed due to the absence of conjugate shears. In these samples, we observed subparallel arrays of compaction bands associated with intensive comminution (corresponding to the dark bands perpendicular to σ_1 in the transmission optical micrographs). The stress-strain curve shows an overall strain hardening trend that is punctuated by episodic stress drops. The number of compaction bands was observed to increase with the cumulative number of stress drops. Such mechanical and microstructural attributes of the Bentheim sandstone are very similar to those of honeycombs that developed compaction bands [*Papka and Kyriakides*, 1998; 1999].

Comparison with localization analysis

Bifurcation analyses [*Rudnicki and Rice*, 1975; *Olsson*, 1999; *Issen and Rudnicki*, 2000] specify the mechanical conditions under which such localized failure modes may develop. The simplest approach is to adopt a constitutive framework whereby the yield envelope and inelastic volumetric change can be characterized by the pressure-sensitivity parameter μ and dilatancy factor β, respectively. Since $\mu=(dQ/dP)/\sqrt{3}$ for axisymmetric compression [*Wong et al.*, 1997], it decreases with increasing P (Figure 1b). The dilatancy factor is given by $\beta=-\sqrt{3}(d\varepsilon_v^p/d\varepsilon_1^p)/(3-d\varepsilon_v^p/d\varepsilon_1^p)$, where $d\varepsilon_v^p/d\varepsilon_1^p$ denotes the ratio between increments of plastic volumetric and axial strains. These parameters were determined following procedures outlined by *Wong et al.* [1997]. Our samples that show localized compactant failure in the transitional regime are all associated with inelastic strain fields with axial shortening $d\varepsilon_1^p>0$ (probably dominated by pore collapse) and lateral expansion $d\varepsilon_2^p=d\varepsilon_3^p<0$ (probably induced by axial microcracking), so that $0<d\varepsilon_v^p<d\varepsilon_1^p$, and accordingly $-\sqrt{3}/2<\beta<0$.

For this simplest model with one yield surface, *Issen and Rudnicki* [2000] derived the general condition $\beta+\mu<-\sqrt{3}$ for inception of compaction band under axisymmetric compression. Given the laboratory constraints $-\sqrt{3}/2<\beta<0$ this model would predict $\mu<-\sqrt{3}/2$ for such samples whereas our measured values were $>-\sqrt{3}/2$ (Figure 4). We attribute the discrepancy to the inadequacy of the constitutive model. The factor β does not adequately account for inelastic volume change induced by the mean stress [*Aydin and Johnson*, 1983]. Microstructrual

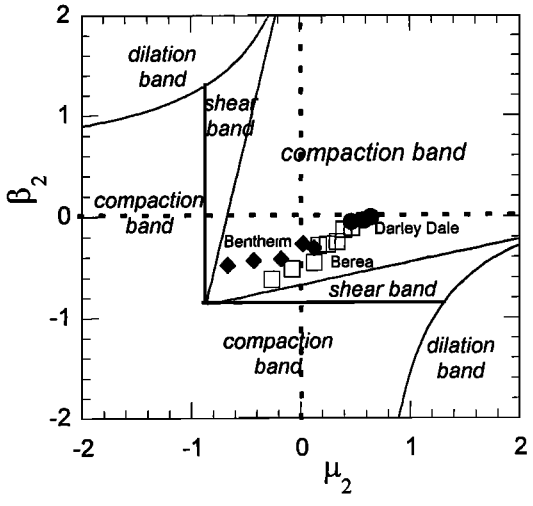

Figure 5. Failure mode map derived from bifurcation analysis of a model with two yield surfaces (from *Issen* [2000]). The analysis is for $(\mu_1-\mu_2)(\beta_1-\beta_2)>0$ and k=0. Constitutive parameters for the Bentheim (dark diamond), Berea (open square) and Darley Dale (dark circle) sandstone samples that failed by development of compaction or high-angle shear bands are also plotted.

observations show that localized failure generally occurs in the transitional regime, that involves the partitioning of damage between at least two mechanism: axial microcracks that may grow and coalesce to form a shear fault, and pores that collapse while grains are crushed. *Issen* [2000] recently proposed a model that incorporates two yield surfaces. The second yield surface is characterized by a pressure-sensitivity factor μ_2, and the relevant plastic deformation is characterized by a dilatancy factor β_2 and a bulk hardening modulus k (related to inelastic volumetric strain induced by mean stress). Whereas the first yield surface represents a dilatant, frictional mechanism with positive μ_1 and β_1, the second yield surface represents a compactant mechanism with negative β_2.

The bifurcation analysis for this more elaborate constitutive model is very involved, but analytic results are available for the limiting case for $(\mu_1-\mu_2)(\beta_1-\beta_2)>0$ and k=0 (which corresponds to the almost flat "shelves" in curves for the transitional regime in Figure 1a). The failure mode map is illustrated in Figure 5, and for comparison constitutive parameters inferred from our data for samples that show localized compactant failure are also plotted. In this model with two yield surfaces, compaction bands may develop over a wide range of μ_2 and β_2, and in this sense the predictions are in better agreement with our mechanical data. Further analyses are required to elucidate the progressive development of the localized failure since the bifurcation analysis applies only to the onset of localization.

Discussion

The porosities of our three sandstones and Castlegate sandstone cover a wide range from 13% to 28%. Localized failure modes involving compaction bands and high-angle conjugate shears have been observed in all these sandstones while undergoing shear-enhanced compaction. Our systematic study has demonstrated that such failure modes are associated with stress states in the transitional regime from brittle faulting to distributed cataclastic flow. The stress states (Figure 1b) are in the range typically encountered in sedimentary formations. The laboratory results therefore suggest that these complex localized features can be pervasive in sandstone formations, not just limited to the very porous aeolian sandstone in which they were first documented [*Mollema and Antonellini*, 1996]. Recognition of such structures in the field would elucidate the complex development of localization in sandstone formation [*Aydin and Johnson*, 1978] and accretionary prism [*Byrne et al.*, 1993].

Future studies should explore whether localized failure modes also develop in other materials such as carbonate rock and soil. While bifurcation theory provides an useful framework for analyzing the inception of localization, our data do not agree with predictions for a constitutive model that does not account for the activation of multiple damage mechanisms in the transitional regime. Reasonable agreement was obtained for the limiting case of a constitutive model that incorporates two yield surfaces, but further theoretical analyses are necessary to clarify the sensitivity of localization inception to the constitutive parameters.

Acknowledgments. We thank Kathleen Issen for sending us a copy of her thesis. We have benefited from discussions with her, John Rudnicki, Pierre Bésuelle, Joanne Fredrich, Yves Guéguen, Mervyn Paterson, and Veronika Vajdova. This research was partially supported by the Office of Basic Energy Sciences, Department of Energy under grant DEFG0299ER14996.

References

Aydin, A., and A.M. Johnson, Analysis of faulting in porous sandstones, *J. Struct. Geol.*, *5*, 19-31, 1983.

Aydin, A., and A.M. Johnson, Development of faults as zones of deformation bands and as slip surfaces in sandstone, *PAGEOPH*, *116*, 931-942, 1978.

Baud, P., W. Zhu, and T.-f. Wong, Failure mode and weakening effect of water on sandstone, *J. Geophys. Res*, *105*, 16371-16390, 2000.

Byrne, T., A. Maltman, E. Stephenson, W. Soh, and R. Knipe, Deformation structures and fluid flow in the toe region of the Nankai accretionary prism, *Proc. of the ODP, Scientific Results*, *131*, 83-192, 1993.

DiGiovanni, A.A., J.T. Fredrich, D.J. Holcomb, and W.A. Olsson, Micromechanics of compaction in an analogue reservoir sandstone, *Proc. 4th North Am. Rock Mech. Symp.*, 1153-1160, 2000.

Fletcher, R.C., and D D. Pollard, Anticrack model for pressure solution surfaces, *Geology*, *9*, 419-424, 1981.

Handin, J., R.V. Hager, M. Friedman, and J.N. Feather, Experimental deformation of sedimentany rock under confining pressure: pore pressure effects, *Bull. Am. Asso. Petrol. Geol.*, *47*, 717-755, 1963.

Hickman, S., R. Sibson, and R. Bruhn, Introduction to special issue: Mechanical involvement of fluids in faulting, *J. Geophys. Res.*, *100*, 12831-12840, 1995.

Issen, K.A., and J.W. Rudnicki, Conditions for compaction bands in porous rock, *J. Geophys. Res.*, *105*, 21529-21536, 2000.

Issen, K.A., Conditions for Localized Deformation in Compacting Porous Rocks, Ph.D. thesis, Northwestern University, Evanston, IL, 2000.

Klein, E., P. Baud, T. Reuschle, and T.-f. Wong, Mechanical behaviour and failure mode of Bentheim sandstone under triaxial compression, in press, *Phys. Chem. Earth (A)*, *26*, 21-25, 2001.

Menéndez, B., W. Zhu, and T.-f. Wong, Micromechanics of brittle faulting and cataclastic flow in Berea sandstone, *J. Struct. Geol.*, *18*, 1-16, 1996.

Mollema, P.N., and M.A. Antonellini, Compaction bands: A structural analog for anti-mode I cracks in aeolian sandstone, *Tectonophysics*, *267*, 209-228, 1996.

Olsson, W.A., and D.J. Holcomb, Compaction localization in porous rock, *Geophys. Res. Lett.*, *27*, 3537-3540, 2000.

Olsson, W.A., Theoretical and experimental investigation of compaction bands in porous rock, *J. Geophys. Res.*, *104*, 7219-7228, 1999.

Papka, S.D., and S. Kyriakides, Biaxial crushing of honeycombs - Part I: Experiments, *Int. J. Solids Struct.*, *36*, 4367-4396, 1999.

Papka, S.D., and S. Kyriakides, Experiments and full-scale numerical simulations of in-plane crushing of a honeycomb, *Acta mater.*, *46*, 2765-2776, 1998.

Paterson, M.S., *Experimental Rock Deformation - The Brittle Field*, 254 pp., Spinger-Verlag, New York, 1978.

Rice, J.R., Fault stress states, pore pressure distributions, and the weakness of the San Andreas fault, in *Fault Mechanics and Transport Properties of Rocks*, edited by B. Evans, and T.-f. Wong, pp. 475-504, Academic Press, San Diego, 1992.

Rudnicki, J.W., and J.R. Rice, Conditions for the localization of deformation in pressure sensitive dilatant materials, *J. Mech. Phys. Solids*, *23*, 371-394, 1975.

Scholz, C.H., *The Mechanics of Earthquakes and Faulting*, 433 pp., Cambridge University Press, Cambridge, 1990.

Wong, T.-f., C. David, and W. Zhu, The transition from brittle faulting to cataclastic flow in porous sandstones: Mechanical deformation, *J. Geophys. Res.*, *102*, 3009-3025, 1997.

Wu, X.Y., P. Baud, and T -f. Wong, Micromechanics of compressive failure and spatial evolution of anisotropic damage in Darley Dale sandstone, *Int. J. Rock Mech. Min. Sci.*, *37*, 143-160, 2000.

Teng-fong Wong, Department of Geosciences, SUNY at Stony Brook, Stony Brook, NY 11794-2100. (e-mail: Teng-fong.Wong@sunysb.edu)

Patrick Baud and Emmanuelle Klein, Institut de Physique du Globe de Strasbourg, 5 rue René Descartes, 67084 Strasbourg, France. (e-mail: Patrick.Baud@eost.u-strasbg.fr, Emmanuelle.Klein@eost.u-strasbg.fr)

(Received 02/03/01; accepted 03/15/01)